Risk of COVID-19 epidemic resurgence with the introduction of vaccination passes

Tyll Krueger[1,*], Krzysztof Gogolewski[2,*], Marcin Bodych[1,*], Anna Gambin[2], Giulia Giordano[3], Sarah Cuschieri[4], Thomas Czypionka[5,6], Matjaz Perc[7,8,9,10], Elena Petelos[11,12], Magdalena Rosińska[13], and Ewa Szczurek[2,†]

[1]*Faculty of Electronics, Department of Control Systems and Mechatronics, Wroclaw University of Science and Technology, Wroclaw, Poland*

[2]*Faculty of Mathematics, Informatics and Mechanics, University of Warsaw, Warszawa, Poland*

[3]*Department of Industrial Engineering, University of Trento, Trento, Italy*

[4]*Department of Anatomy, Faculty of Medicine and Surgery, University of Malta, Msida, Malta*

[5]*Institute for Advanced Studies, Josefstädterstraße 39, 1080, Vienna, Austria*

[6]*London School of Economics and Political Science, Houghton Street, WC2A 2AE, London, UK.*

[7]*Faculty of Natural Sciences and Mathematics, University of Maribor, Koroška cesta 160, 2000 Maribor, Slovenia*

[8]*Complexity Science Hub Vienna, Josefstädterstraße 39, 1080 Vienna, Austria*

[9]*Department of Medical Research, China Medical University Hospital, China Medical University, Taichung 404332, Taiwan*

[10]*Alma Mater Europaea, Slovenska ulica 17, 2000 Maribor, Slovenia*

[11]*Clinic of Social and Family Medicine, Faculty of Medicine, University of Crete, Heraklion, Greece.*

[12]*Department of Health Services Research, CAPHRI-Care and Public Health Research Institute, Maastricht University, Maastricht, The Netherlands*

[13]*Department of Infectious Disease Epidemiology and Surveillance, National Institute of Public Health, Warsaw, Poland.*

[*]*Shared first authorship*

[†]*Correspondence: szczurek@mimuw.edu.pl*

Many countries hit by the COVID-19 epidemic consider the introduction of vaccination passes. So far, no thorough impact assessment of vaccination passes and of lower restrictions for their holders has been conducted. Here, we propose the VAP-SIRS model that accounts for susceptible, infected, and recovered subpopulations, also within the group of vaccinated pass holders. The model accounts for imperfect vaccination effectiveness, revaccinations and waning immunity. Different restrictions for pass holders and the rest of the population result in different scenarios of the epidemic evolution, some of which yield unfavourable COVID-19 dynamics and new waves. We identify critical variables that should be considered by policymakers and show how unfavourable outcomes can be avoided using adaptive policies. In particular, while pass holders could initially be allowed large freedoms, the gradual loss of immunity will require either increased restrictions for pass holders, or accelerated revaccination. In the long-term, common restrictions for both the pass holders and the rest of the population will have to be kept to avoid epidemic resurgence. Such minimum required restrictions depend on vaccination effectiveness, revaccination rate, waning rate and fraction of never-vaccinated population, and, for realistic combinations of these parameters, range between 29% and 69% reduction of contacts.

Main

In the past, governments have required proof of vaccination for travel, with yellow fever being the best-known example, and the only disease for which a certificate is needed to cross borders in compliance to the International Health Regulations[1]. However, the idea that proof of vaccination will become a prerequisite for crossing borders or to enter facilities, visit businesses premises, participate in events, and generally enjoy more freedom, has only arisen in the context of combatting the COVID-19 epidemic. Despite technical challenges, scientific uncertainties, and ethical and legal dilemmas, the idea of vaccination passes (VPs), i.e., documents issued on the basis of vaccination status, is now receiving unprecedented attention[2,3,4]. Many consider VPs as tools to restore people's freedoms and increase well-being, whilst allowing economies to reopen. Determining immunity status is challenging, as the immune response and its dura-

tion may greatly vary; this being applicable to post-vaccination immunity, as well as following natural SARS-CoV-2 infection and recovery[5]. It is, therefore, critically important to determine levels of restrictions that offer safety whilst being tolerable, ensuring good compliance and rational behaviour. Less than perfect conferred protection coupled with suboptimal levels of restrictions can have detrimental effects. The lack of a comprehensive framework to determine such levels, including when approaching higher vaccination coverage and even herd immunity, may result in policymakers opting to select suboptimal levels of restrictions. This may happen for different reasons, such as lack of true understanding of the ramifications, to boost morale or, even, for political gain. Evidence indicates vaccine effectiveness can greatly vary[6,7] and it may be compromised due to escape variants[8] and waning immunity[9,10,11,12].

Various models have been developed to inform vaccination strategies[13,14,15,16,17,18,19,20,21]. One such effort indicates lower vaccine effectiveness coupled with an increase in social contact among those vaccinated (behavioral compensation) may undermine vaccination effects, even without considering immunity waning[22]. So far, there has been no model to focus on the medium- and long-term impact of relaxing restrictions for VP holders, with due consideration to vaccine effectiveness, durability of response, and vaccine hesitancy. The proposed VAP-SIRS model delivers a systematic framework to assess key considerations for policymaking.

Results

The VAP-SIRS model of the impact of COVID-19 vaccination passes

The VAP-SIRS model extends the classical SIRS model[23] (red arrows in Fig. 1a) with additional states and parameters that describe the dynamics of vaccination routine in a population (green arrows in Fig 1a.). To this end, we consider the following subpopulations: (i) initially susceptible S_N, who, if successfully vaccinated, populate the immune group V, with rate av, where v is the vaccination rate and a is the effectiveness, (ii) susceptible who were vaccinated but did not gain immunity (S_1), (iii) vaccinated, whose immunity waned with rate ω and became susceptible again (S_2), (iv) susceptible, who are not and will never get vaccinated (S_D). Additionally, revaccination of S_2 populates V with rate av_r. All recovered, unless recovered

compartment R_D, are also subject to vaccination. The fraction of the population that will never be vaccinated is denoted d.

The presented model analysis is performed for carefully selected parameter setups: two different vaccination rates, 0.004 and 0.008 dose per person daily, chosen on the basis of the current rates observed in Europe[24,25], and for vaccine effectivenesses 0.6 and 0.9, which conservatively model that of the most widely used vaccines: Vaxzevria (AstraZeneca)[26,27] and Comirnaty (BioNTech/Pfizer)[28,7,29], respectively. Furthermore, optimistic (500 days; $\omega = 1/500$) and pessimistic (200 days; $\omega = 1/200$) average immunity duration periods are considered, reflecting emerging data on large individual variation of immunity waning and other key factors influencing this process[9,12,30,31,32]. Finally, across the manuscript, we assume the revaccination rate $\upsilon_r = \upsilon$, and consider optimistic 0.1, and pessimistic 0.3 fractions of never-vaccinated d .

We assume that VP holders are all who were vaccinated at least once (Fig. 1). The restriction level f (ranging from 0 to 1) is introduced as a modulator of the SARS-CoV-2 reproduction number. Here, we consider that without any restrictions ($f = 0$), the reproduction number for the virus equals 4, as an optimistic estimate for B.1.1.7[33,34]. Similarly, restrictions $f_{\mathrm{v}} \leq f$ for contacts among VP holders are considered. f and f_{v} should be interpreted as the net effect of all factors that reduce the reproduction number of the virus within the respective groups: all applied non-pharmaceutical interventions together with the resulting changes in behavior. Based on the current studies, we fix the generation time to 6 days ($\gamma = 1/6$)[34,33]. Finally, we consider two types of mixing between subpopulations: proportional (typical for SIR models) and preferential, where the VP holders prefer contacts with other VP holders. See Methods for a detailed model description.

VAP-SIRS predicts a possible infection resurgence despite vaccinations

VAP-SIRS predicts unfavourable epidemic dynamics for a wide range of parameters. As an example consider: $a = 0.9$, $\upsilon = \upsilon_r = 0.004$, $d = 0.1$, and $\omega = 1/500$, a seemingly safe setup, which we will call the reference setup. For such setup and low restrictions $f_{\mathrm{v}} = 0.05$ for VP holders as well as medium restrictions $f = 0.63$ for contacts with and within the rest of the population, the model predicts a small wave of infections shortly after the vaccination

program starts, followed by a large wave later (Fig. 1b). This behavior is explained by the population structure and different restrictions (Fig. 1c). In this scenario, the first wave is driven by the unvaccinated susceptibles (S_N) and suppressed by ongoing vaccination, as expected. Interestingly, the second, larger wave is driven by the S_V group. The S_V group is composed of the number of individuals for whom the vaccine was ineffective (S_1) and those vaccinated who lose their immunity and are not yet revaccinated (S_2). In the following we investigate how the dynamics change for different restrictions settings.

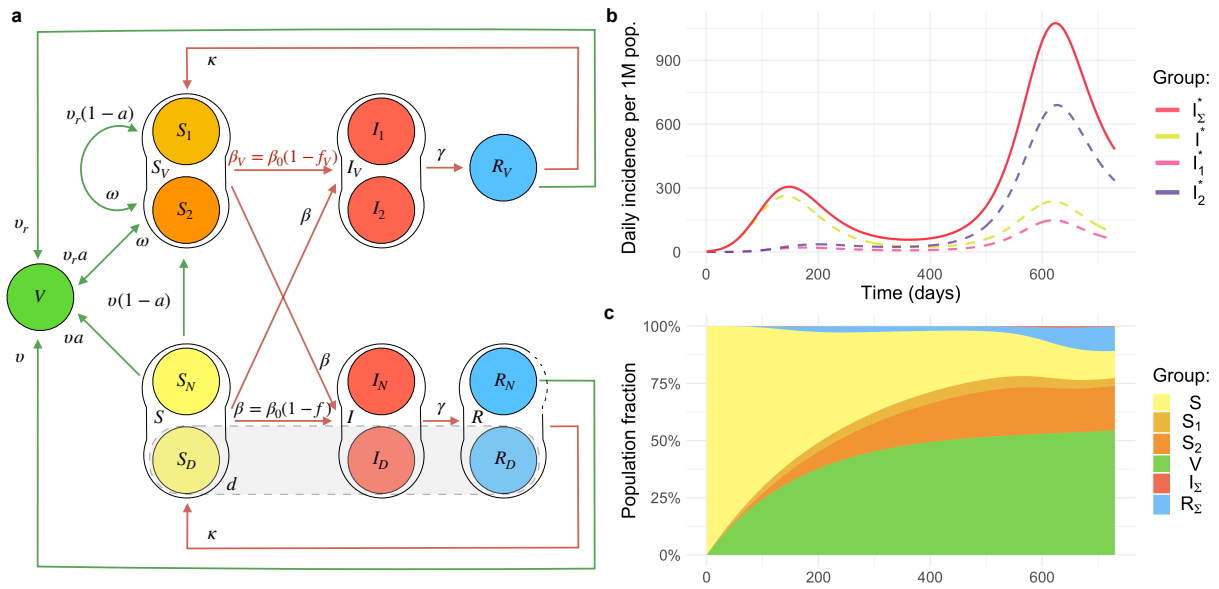

Figure 1: **The VAP-SIRS model shows the possible rebound of infections after a large population is vaccinated and obtains a VP, but then loses immunity. a.** Graphical scheme of the VAP-SIRS model. **b.** The timeline of daily incidence per 1 million inhabitants for an effective vaccine (a = 0.9), slow (re-)vaccination rate ($\upsilon = \upsilon_r = 0.004$; typical for many European countries), proportional mixing (see Methods) and low fraction of never-vaccinated ($d = 0.1$). Here, a variable with the asterisk (*) indicates that we consider a daily incidence over the corresponding variable, thus I^* stands for $I^*_D + I^*_N$, and by I^*_Σ we mean the sum of all daily infected ($I^* + I^*_1 + I^*_2$). **c.** The Muller plot of the population structure (the width of the color band in the y axis) as a function of time (x axis) for the same parameter settings as in **b.** Here, by I_Σ and R_Σ we denote $I + I_V$ and $R + R_V$, respectively.

Stability analysis identifies potential scenarios for the COVID-19 epidemic depending on the restrictions imposed on VP holders and the rest of the population.

To assess the epidemic evolution in different scenarios, we analysed stability by linearising the model equations with $I = R = 0$ (Methods). The restriction levels $\mathbf{f} = (f, f_{\mathrm{v}})$ influence the *instantaneous reproduction number* R^*. $R^*(t)$ is the reproduction number that would be observed at time t, given the restrictions $\mathbf{f}$ and the composition of the population, where the number of infected is very small. If $R^*(t) > 1$, then switching to $\mathbf{f}$ at time t results in an *overcritical* epidemic evolution, with an initially exponential growth of infections; if $R^*(t) < 1$, switching to $\mathbf{f}$ at time t results in a *subcritical* epidemic evolution, where the number of active cases decreases to zero. The R^* is more informative of epidemic thresholds than the standard effective reproduction number, as it does not depend on the actual number of infected and recovered.

We consider five restriction choices (prototypical for five regions of the parameter space), leading to different time profiles of R^* (Fig. 2a). Medium restrictions for both VP holders and the rest of the population (red curve in Fig. 2a) lead to an overcritical epidemic. Medium restrictions for VP holders and strong restrictions for the others (blue curve in Fig. 2a) lead to a subcritical epidemic. With low restrictions for VP holders and medium restrictions for the rest of the population (orange curve in Fig. 2a), the epidemic is initially overcritical, becomes subcritical and then switches to overcritical again; this is the scenario shown in the simulation in Fig. 1b,c. With very low restrictions for VP holders and strong restrictions for the rest of the population (pink curve in Fig. 2a), the epidemic is initially subcritical and then becomes overcritical. If low restrictions are adopted for VP holders and medium restrictions for the rest of the population (cyan curve in Fig. 2a), the epidemic is initially overcritical and then switches to subcritical.

In each scenario we computed the time evolution of the *instantaneous doubling time* D (Methods). For a given $\mathbf{f}$, $D(t)$ is the doubling time (capturing how fast the infections grow) that would be observed for the growth of a small initial number of infections at time t, with

enforced restrictions f. Very short doubling times, below 30 days, can be observed in three scenarios that are (eventually) overcritical: see the red, orange and pink curves in Fig. 2b.

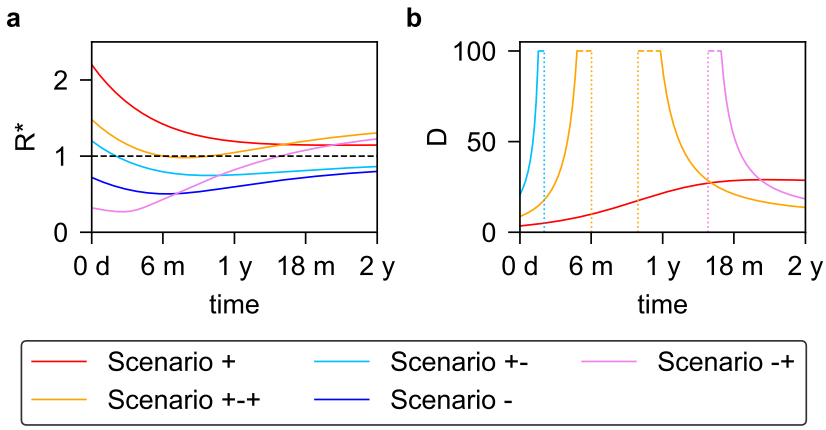

Figure 2: **Intensity and timing of the infection wave: examples of five scenarios depending on the restrictions for VP holders and for the rest of the population.** Given $a = 0.9$, $\upsilon = \upsilon_r = 0.004$, $\omega = 0.002$, $d = 0.1$ and proportional mixing, we compare five different scenarios describing the epidemic evolution: overcritical (+, red, $f = 0.45$ and $f_\mathrm{v} = 0.32$), subcritical (−, blue, $f = 0.82$ and $f_\mathrm{v} = 0.4$), initially and eventually overcritical (+−+, orange, $f = 0.63$ and $f_\mathrm{v} = 0.05$), eventually overcritical (−+, pink, $f = 0.92$ and $f_\mathrm{v} = 0.04$), eventually subcritical (+−, cyan, with $f = 0.7$ and $f_\mathrm{v} = 0.4$). **a.** Time evolution of R^* (y axis) depending on the number of days counted from the start of the vaccination program (x axis). **b.** Doubling time D (y axis, in days) as a function of the number of days (x axis). Note that doubling curves are cut above 100 days, in the time intervals indicated by the horizontal dashed lines. Negative doubling times (halving times) are not plotted. Thus, the subcritical scenario (−) is not visualised in **b.** Vertical dotted lines indicate the times at which a transition occurs from overcritical to subcritical, or vice versa.

Different restrictions are required to avoid epidemic resurgence depending on parameter setups

The relevant $f - f_\mathrm{v}$ parameter space, where $f_\mathrm{v} \leq f$, can be divided into five regions, where the epidemic dynamics follows the distinct patterns exemplified in Figure 2. The area occupied by each region changes depending on the parameter setups, as shown in Figure 3. For example, in the reference setup in Figure 3a (high vaccine effectiveness $a = 0.9$ and (re-)vaccination rates $\upsilon = \upsilon_r = 0.004$, low never-vaccinated fraction $d = 0.1$ and low immunity waning rate $\omega = 0.002$), the overcritical region (with R^* always above 1) occupies the lower left corner. It is enlarged with smaller vaccine effectiveness (a = 0.6, Fig. 3b), larger fraction of the never-

vaccinated population (Fig. 3e) and higher waning rate (Fig. 3f), while it shrinks with higher vaccination rate (Fig. 3c). The subcritical region - (with R^* always smaller than 1) lies in the opposite corner of the $f - f_\mathrm{v}$ space, for larger values, and for a fixed fraction of never-vaccinated d tends to decrease for setups where the overcritical region increases. Inside each of the remaining three regions (associated with the $+-+$, $-+$, $+-$ scenarios in Figure 2), the specific parameter settings differ by the time to the critical threshold of interest for that region (the last observed switch between subcritical and overcritical epidemic, which for the $+-+$ region, for example, is the second critical threshold; see Methods for the computation of the times to critical thresholds). For the reference setup (Fig. 3a), the critical threshold is reached after a minimum ~ 8 months. Decreasing vaccine effectiveness (Fig. 3b), as well as increasing the waning rate (Fig. 3f), enlarges the $+-+$ region' and leads to overcriticality sooner, after ~ 3 and ~ 4 months respectively, for low f_v values. Increasing vaccination rate (Fig. 3c) shrinks the $+-+$ region. With preferential mixing (Fig. 3d), the $+-+$ region becomes larger and overcriticality is reached even sooner. Increasing the number of never-vaccinated people (Fig. 3e) shrinks the $+-+$ region and delays the onset of overcriticality. For all considered parameter setups, except for the one with high (re-)vaccination rate, for all except the $+-$ and the $-$ regions, large asymptotic R^* can be expected, which corresponds to short doubling times (Fig. 3).

These results indicate that VP holders can be granted large freedom, as long as sufficient restrictions are enforced for the rest of the population, to avoid an initially overcritical situation. However, to prevent the epidemic from becoming overcritical after an initial decline in case numbers, restrictions on VP holders need to be timely increased and adapted so that eventually everyone faces the same restrictions. Safe restrictions correspond to the parameters in the subcritical region, but these are relatively high and could be unacceptable for the population. The $-+$ and $+-+$ regions can seem attractive from the aspect of large freedom for the VP holders. Both these regions, however, eventually result in epidemic resurgence and should be avoided. Moving to the $+-$ region with the right timing is a recommendable strategy.

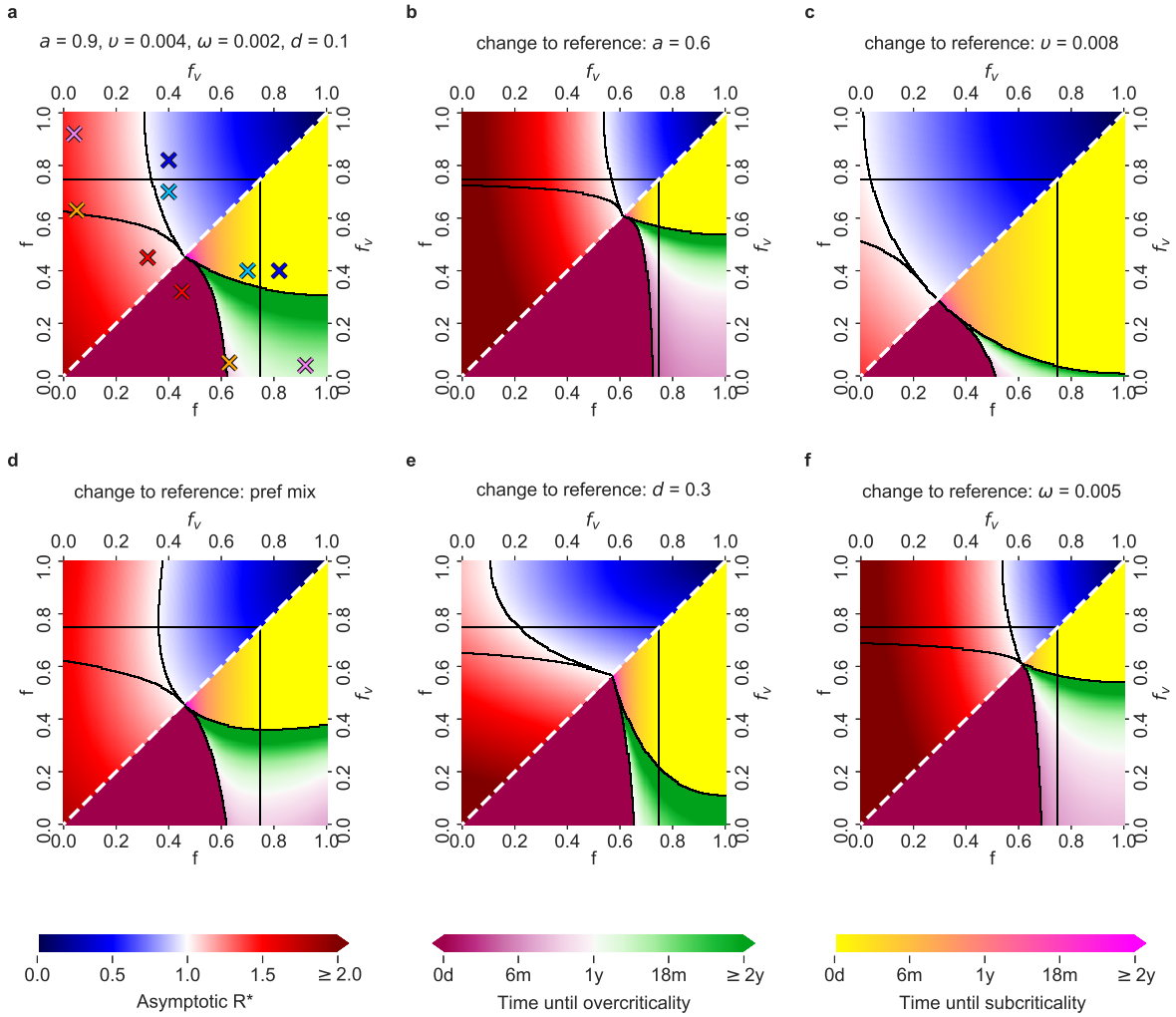

Figure 3: **Possible COVID-19 epidemic dynamics depending on vaccine effectiveness, vaccination rate, mixing type and the restrictions for VP holders and for the rest of the population.** For various choices of the other parameters, the relevant $f - f_{\mathrm{v}}$ parameter space, where $f_{\mathrm{v}} \leq f$, can be divided into five regions, each associated with a different behavior of the epidemic, exemplified by the five scenarios in Figure 2a. On the diagonal (white dashed line), $f = f_{\mathrm{v}}$, namely the restrictions for VP holders and for the rest of the population are the same. Lower triangles show the time until the last critical threshold: different colour scales correspond to the time until the switch either from a subcritical to an overcritical epidemic (time until overcriticality, violet-green scale), or from an overcritical to a subcritical epidemic (time until subcriticality, yellow-pink scale). Upper triangles show the asymptotic R^*, as a function of the values of f and f_{v} (blue-red scale, with blue associated with $R^* < 1$ and red associated with $R^* > 1$). **a.** Reference setup, with $a = 0.9$, $\upsilon = \upsilon_r = 0.004$, $\omega = 0.002$, $d = 0.1$ and proportional mixing. The choices of (f, f_{v}) corresponding to the five scenarios exemplified in Figure 2 are denoted by crosses of the same colour. **b.** Setup with decreased vaccine effectiveness: $a = 0.6$. **c.** Setup with increased vaccination rate: $\upsilon = \upsilon_r = 0.008$. **d.** Setup with preferential (instead of proportional) mixing. **e.** Setup with increased fraction of people who will not get vaccinated: $d = 0.3$. **f.** Setup with increased waning rate: $\omega = 0.005$.

A minimum common restriction level is required to keep the epidemic subcritical

We compute the minimum common restriction level $f_{\min}$ for the whole population that would be required to avoid an overcritical epidemic in the long-term (Methods):

$$f_{\min} = \max(0, 1 - 1/(4 \cdot (1 - V^{\text{as}})),$$

where V^{as} is the asymptotic fraction of the immunized in the population

$$V^{\text{as}} = (1 - d)\frac{a}{1 + \omega/\upsilon_r}.$$

The resulting values differ depending on the setups of vaccine effectiveness a, revaccination rate υ_r, the fraction of never-vaccinated population d and immunity waning rate ω (Tab. 1). Even for the most optimistic setup (high a = 0.9, high $\upsilon_r = 0.008$, low $d = 0.1$, low $\omega = 0.002$) we obtain $V^{\text{as}} = 0.65$, and $f_{\min} = 0.29$. Compared to the current strict restrictions required to contain COVID-19 in some countries, the level of 0.29 restrictions is lower, but it is a considerable reduction of freedom compared to before the pandemic. All remaining realistic parameter setups require high $f_{\min}$, ranging between 0.46 (for the reference setup) and 0.68 (for the increased d, increased ω as compared to the reference).

Discussion

Introducing VPs is widely seen as a means to opening up economies and societies, despite the ongoing epidemic. To inform this discussion, we extend a SIR model to reflect vaccination dynamics and possibly different restrictions for VP holders. A wide range of model parameter choices show the possibility of an epidemic resurgence, even for optimistic parameter setups. The main driver of this phenomenon is the potential lack of immunity of VP holders. With a VP, people enjoy low restrictions while actually being susceptible and potentially contagious because the vaccine was ineffective or the immunity has waned.

VAP-SIRS deliberately keeps several aspects simple (see Methods for model limitations).

	Parameter setup	a	υ_r	d	ω	V^{as}	f_{min}
1	Reference setup (ref Fig. 3a)	0.9	0.004	0.1	0.002	0.54	0.46
2	Decreased a (ref Fig. 3b)	**0.6**	0.004	0.1	0.002	0.36	0.61
3	Increased υ_r (ref Fig. 3c)	0.9	**0.008**	0.1	0.002	0.65	0.29
4	Increased d (ref Fig. 3e)	0.9	0.004	**0.3**	0.002	0.42	0.57
5	Increased ω (ref Fig. 3f)	0.9	0.004	0.1	**0.005**	0.36	0.61
6	Decreased a and increased υ_r	**0.6**	**0.008**	0.1	0.002	0.43	0.56
7	Decreased a and increased d	**0.6**	0.004	**0.3**	0.002	0.28	0.65
8	Decreased a and increased ω	**0.6**	0.004	0.1	**0.005**	0.24	0.67
9	Increased υ_r, increased d	0.9	**0.008**	**0.3**	0.002	0.50	0.50
10	Increased υ_r, increased ω	0.9	**0.008**	0.1	**0.005**	0.50	0.50
11	Increased d, increased ω	0.9	0.004	**0.3**	**0.005**	0.21	0.68

Table 1: **Asymptotic level of immunization V^{as} and minimum common restrictions f_{min} for different parameter setups**, for parameters: vaccine effectiveness a, revaccination rate υ_r, fraction of never-vaccinated d, and waning immunity rate ω. The first row concerns the reference setup; rows below are setups with the same parameters as in the reference setup, but with either one parameter changed (in bold; rows 2–5; same as in Figure 3, apart from preferential mixing, as it is not relevant for common restrictions) or two parameters changed (in bold; rows 6–11).

The advantage of our analysis is the relevance for long-term dynamics, and the focus on avoiding epidemic resurgence. Avoiding another wave is a prudent goal due to threats it poses, in the form of long-term health effects, the deleterious impact on societies and the emergence of new variants.

Our model gives valuable insights into policies pertaining to the introduction of VPs. Model analyses suggest that considerably lowering restrictions for VP holders is only possible when keeping high restrictions on the rest of the population. This situation seems tolerable for the unvaccinated only given high vaccine availability and vaccination speed. The alternative cautious option, i.e. not granting freedoms for VP holders, defeats the purpose of the instrument. Once a large part of the population has been vaccinated, policymakers need to find a new, common restriction level, which could also be achieved through temporary VPs. Our model implies that such common restrictions need to be higher than those initially granted to VP holders, and need to be introduced in time to avoid another wave.

As expected, the model shows that there is a larger selection of admissible restrictions' setups under high vaccine effectiveness, slowly waning immunity, proportional social mixing, low share of never-vaccinated and higher vaccination rate. At least the latter two parameters are amenable to policy action. Thus, efforts to increase (re-) vaccination speed and encour-

age people to get vaccinated also extend the margin of lowering restrictions for VP holders as well as eventual common restrictions. Social mixing patterns, such as preferential mixing, can accelerate the infection resurgence in time and, although difficult to change by policymaking, should be monitored. Finally, it is noteworthy that VP holders are less likely to be tested, as they are assumed to be protected and they may exhibit milder symptoms. Therefore, their potential infection is more likely to remain undetected, resulting in an effect similar to that of lowering restrictions. To prevent undesirable outcomes, the testing criteria should not exclude the VP holders. In addition, the VP holders should be widely and regularly tested for antibody level, aiming at detection of such vaccinated that have lost, or have never gained, immunity. Finally, temporary VPs could be considered, with their prolongation conditioned on high antibody level or recent (re-)vaccination.

References

1. *International health regulations (2005)* Third edition (ed World Health Organization) (World Health Organization, Geneva, Switzerland, 2016).

2. Voo, T. C. *et al.* Immunity certification for COVID-19: ethical considerations. *Bulletin of the World Health Organization* **99,** 155–161 (2021).

3. Brown, R. C. H., Kelly, D., Wilkinson, D. & Savulescu, J. The scientific and ethical feasibility of immunity passports. *The Lancet Infectious Diseases* **21,** e58–e63 (2021).

4. European Commission, Directorate-General for Justice and Consumers. *Proposal for a REGULATION OF THE EUROPEAN PARLIAMENT AND OF THE COUNCIL on a framework for the issuance, verification and acceptance of interoperable certificates on vaccination, testing and recovery to facilitate free movement during the COVID-19 pandemic (Digital Green Certificate, Document 52021PC0130)* https://eur-lex.europa.eu/legal-content/EN/TXT/?uri=CELEX:52021PC0130 (2021).

5. World Health Organization. *"Immunity passports" in the context of COVID-19* tech. rep. (WHO). https://www.who.int/news-room/commentaries/detail/immunity-passports-in-the-context-of-covid-19 (2021).

6. Voysey, M. *et al.* Single-dose administration and the influence of the timing of the booster dose on immunogenicity and efficacy of ChAdOx1 nCoV-19 (AZD1222) vaccine: a pooled analysis of four randomised trials. *The Lancet* **397,** 881–891 (2021).

7. Thompson, M. G. *et al.* Interim Estimates of Vaccine Effectiveness of BNT162b2 and mRNA-1273 COVID-19 Vaccines in Preventing SARS-CoV-2 Infection Among Health Care Personnel, First Responders, and Other Essential and Frontline Workers — Eight U.S. Locations, December 2020–March 2021. *MMWR. Morbidity and Mortality Weekly Report* **70,** 495–500 (2021).

8. Bian, L. *et al.* Effects of SARS-CoV-2 variants on vaccine efficacy and response strategies. *Expert Review of Vaccines,* 1–9 (2021).

9. Chia, W. N. *et al.* Dynamics of SARS-CoV-2 neutralising antibody responses and duration of immunity: a longitudinal study. *The Lancet Microbe.* https://doi.org/10.1016/s2666-5247(21)00025-2 (2021).

10. Iyer, A. S. *et al.* Persistence and decay of human antibody responses to the receptor binding domain of SARS-CoV-2 spike protein in COVID-19 patients. *Science Immunology* **5,** eabe0367 (2020).

11. Hall, V. J. *et al.* SARS-CoV-2 infection rates of antibody-positive compared with antibody-negative health-care workers in England: a large, multicentre, prospective cohort study (SIREN). *The Lancet* **397,** 1459–1469 (2021).

12. Hansen, C. H., Michlmayr, D., Gubbels, S. M., Mølbak, K. & Ethelberg, S. Assessment of protection against reinfection with SARS-CoV-2 among 4 million PCR-tested individuals in Denmark in 2020: a population-level observational study. *The Lancet* **397,** 1204–1212 (2021).

13. Sadarangani, M. *et al.* Importance of COVID-19 vaccine efficacy in older age groups. *Vaccine* **39,** 2020–2023 (2021).

14. Prieto Curiel, R. & González Ramírez, H. Vaccination strategies against COVID-19 and the diffusion of anti-vaccination views. *Scientific Reports* **11,** 6626 (2021).

15. Moore, S., Hill, E. M., Tildesley, M. J., Dyson, L. & Keeling, M. J. Vaccination and non-pharmaceutical interventions for COVID-19: a mathematical modelling study. *The Lancet Infectious Diseases* (2021).

16. Lee, B. Y. *et al.* Vaccination Deep Into a Pandemic Wave. *American Journal of Preventive Medicine* **39,** e21–e29 (2010).

17. Jentsch, P. C., Anand, M. & Bauch, C. T. Prioritising COVID-19 vaccination in changing social and epidemiological landscapes: a mathematical modelling study. *The Lancet Infectious Diseases* (2021).

18. Bubar, K. M. *et al.* Model-informed COVID-19 vaccine prioritization strategies by age and serostatus. *Science* **371,** 916–921 (2021).

19. Bauer, S. *et al.* Relaxing restrictions at the pace of vaccination increases freedom and guards against further COVID-19 waves in Europe. *arXiv:2103.06228 [q-bio].* arXiv: 2103.06228. http://arxiv.org/abs/2103.06228 (2021).

20. Giordano, G. *et al.* Modeling vaccination rollouts, SARS-CoV-2 variants and the requirement for non-pharmaceutical interventions in Italy. *Nature Medicine* (2021).

21. Moghadas, S. M. *et al.* Evaluation of COVID-19 vaccination strategies with a delayed second dose. *PLOS Biology* **19** (ed Read, A. F.) e3001211 (2021).

22. Makhoul, M. *et al.* Epidemiological Impact of SARS-CoV-2 Vaccination: Mathematical Modeling Analyses. *Vaccines* **8,** 668 (2020).

23. Keeling, M. J. & Rohani, P. *Modeling Infectious Diseases in Humans and Animals* (2021) (Princeton University Press, Sept. 2011).

24. Ritchie, H. *et al. Coronavirus (COVID-19) Vaccinations* https://ourworldindata.org/covid-vaccinations (2021).

25. European Centre for Disease Prevention and Control (ECDC). *COVID-19 Vaccine Tracker* https://vaccinetracker.ecdc.europa.eu/public/extensions/COVID-19/vaccine-tracker.html (2021).

26. Hung, I. F. N. & Poland, G. A. Single-dose Oxford–AstraZeneca COVID-19 vaccine followed by a 12-week booster. *The Lancet* **397,** 854–855 (2021).

27. Emary, K. R. W. *et al.* Efficacy of ChAdOx1 nCoV-19 (AZD1222) vaccine against SARS-CoV-2 variant of concern 202012/01 (B.1.1.7): an exploratory analysis of a randomised controlled trial. *The Lancet* **397,** 1351–1362 (2021).

28. Polack, F. P. *et al.* Safety and Efficacy of the BNT162b2 mRNA Covid-19 Vaccine. *New England Journal of Medicine* **383,** 2603–2615 (2020).

29. Dagan, N. *et al.* BNT162b2 mRNA Covid-19 Vaccine in a Nationwide Mass Vaccination Setting. *New England Journal of Medicine* **384,** 1412–1423 (2021).

30. Letizia, A. G. *et al.* SARS-CoV-2 seropositivity and subsequent infection risk in healthy young adults: a prospective cohort study. *The Lancet Respiratory Medicine* (2021).

31. Rockstroh, A. *et al.* Correlation of humoral immune responses to different SARS-CoV-2 antigens with virus neutralizing antibodies and symptomatic severity in a German COVID-19 cohort. *Emerging Microbes & Infections* **10,** 774–781 (2021).

32. Wajnberg, A. *et al.* Robust neutralizing antibodies to SARS-CoV-2 infection persist for months. *Science* **370,** 1227–1230 (2020).

33. The COVID-19 Genomics UK (COG-UK) consortium *et al.* Assessing transmissibility of SARS-CoV-2 lineage B.1.1.7 in England. *Nature* (2021).

34. Davies, N. G. *et al.* Estimated transmissibility and impact of SARS-CoV-2 lineage B.1.1.7 in England. *Science* **372,** eabg3055 (2021).

Methods

Mathematical model

We introduce a modified susceptible-infectious-recovered-susceptible (SIRS) model [1] (Figure 1a). The population is divided into two subpopulations: those who are not vaccinated (S, I, R) and those who got vaccinated at least once (S_V, I_V, R_V, V). We assume that the group of non-vaccinated susceptible individuals S (and, similarly, infected I and recovered R) is divided into two subgroups: S_N and S_D. The S_N compartment contains such susceptible who will eventually be vaccinated, while those in S_D will not. The S_D compartment contains not only the subpopulation of children, who are currently not included in the vaccination program, but also those who for health reasons cannot be vaccinated, and finally, individuals who do not vaccinate because of hesitancy.

The S_N population is vaccinated with rate υ and effectiveness a. Consequently, the individuals from the S_N group populate the vaccinated group V with rate $a\upsilon$. The individuals in V are considered immune, and we assume that immunization prevents them both from getting infected and infecting others. The S_V compartment is composed of S_1 and S_2 (and, similarly, vaccinated infected I_V consists of I_1 and I_2). Due to vaccine ineffectiveness, people in S_1 are perceived as immunized, but in fact are susceptible. S_1 is populated from S_N with rate $(1-a)\upsilon$. The vaccinated from the V group move to the S_2 group of susceptibles with immunity waning rate ω. The individuals from the S_1 group move to S_2 with the same rate ω. The S_2 group is the group of vaccinated, but no longer immune, and thus, susceptible individuals. In contrast to S_1, we consider that the S_2 group is subject to revaccination. Consequently, a fraction of size a of the population from S_2 populates V with rate $a\upsilon_r$ and a fraction of size $(1-a)$ populates S_1 with rate $(1-a)\upsilon_r$. Across the manuscript, we assume $\upsilon_r = \upsilon$, but the model is general and different values can be considered. Individuals from S_1 move to S_2 with rate ω to ensure that the ineffectively vaccinated are revaccinated with the same speed as the ones for which the vaccine was effective.

Some of the susceptibles in S_1 (or, similarly, S_2) may not get revaccinated fast enough and may become infected and populate I_1 (or, I_2). Then, as in the classical SIRS model, the I_1 (or

I_2) population recovers and populates group R_V with rate γ. We consider that the recovered in R_V may also lose the immunity, and become susceptible again and move to S_2 with rate κ. We fix κ to 0.002, corresponding to average 500 days duration of natural immunity. There remains uncertainty regarding the waning time for natural immunity, but early evidence indicates it lasts at least 180 days [2, 3, 4]. Hence, we assume an optimistic scenario of natural immunity lasting similarly long as the immunity gained via vaccination. Before the recovered in the R_V lose immunity, they might be revaccinated, and, thus, populate the V group with rate υ_r.

The remaining susceptible subgroups (the S_N and S_D) may undergo the same classical dynamics, i.e., become infected, recover, and either become susceptible again or, in case of the recovered in the R_N subgroup, become vaccinated with rate υ.

Note that for the recovered in the R_V or R_N groups we assume that vaccination effectiveness is 1, which is substantiated on the basis of the fact that vaccination combined with a previous infection should confer a much stronger protection than only vaccination of a susceptible individual. The following parameters are used to describe population dynamics in the model:

f_{v}, f	:	restrictions level (for VP holders and others)
β_0	:	basic transmission rate
$\beta_{\mathrm{v}}, \beta$	:	transmission rate (for VP holders and others)
γ	:	recovery rate
κ	:	natural immunity waning rate
a	:	vaccination effectiveness
υ	:	vaccination rate
υ_r	:	revaccination rate
ω	:	vaccine-induced immunity waning rate
d	:	fraction of population that will never get vaccinated

Finally, the following set of ordinary differential equations (ODEs) defines the dynamics

$$
\begin{aligned}
\frac{d}{dt}S_D &= -\left(\beta I + \beta I_V\right) S_D + \kappa R_D, \\
\frac{d}{dt}S_N &= -\left(\beta I + \beta I_V\right) S_N - \upsilon S_N + \kappa R_N, \\
\frac{d}{dt}S_1 &= \upsilon_r \left(1-a\right) S_2 + \upsilon \left(1-a\right) S_N - \omega S_1 - \left(\beta I + \beta_{\mathrm{v}} I_V\right) S_1, \\
\frac{d}{dt}S_2 &= -\upsilon_r S_2 + \omega V + \omega S_1 - \left(\beta I + \beta_{\mathrm{v}} I_V\right) S_2 + \kappa R_V, \\
\frac{d}{dt}V &= \upsilon a S_N + \upsilon_r a S_2 - \omega V + \upsilon_r R_V + \upsilon R_N, \\
\frac{d}{dt}I_D &= \left(\beta I + \beta I_V\right) S_D - \gamma I_D, \\
\frac{d}{dt}I_N &= \left(\beta I + \beta I_V\right) S_N - \gamma I_N, \\
\frac{d}{dt}I_1 &= \left(\beta I + \beta_{\mathrm{v}} I_V\right) S_1 - \gamma I_1, \\
\frac{d}{dt}I_2 &= \left(\beta I + \beta_{\mathrm{v}} I_V\right) S_2 - \gamma I_2, \\
\frac{d}{dt}R_V &= \gamma I_V - \kappa R_V - \upsilon_r R_V, \\
\frac{d}{dt}R_D &= \gamma I_D - \kappa R_D, \\
\frac{d}{dt}R_N &= \gamma I_N - \kappa R_N - \upsilon R_N,
\end{aligned}
\tag{1}
$$

where also the following relations hold

$$
\begin{aligned}
S_V &= S_1 + S_2, \\
I_V &= I_1 + I_2, \\
S &= S_D + S_N, \\
I &= I_D + I_N, \\
R &= R_N + R_D,
\end{aligned}
$$

with the constraint $S, S_V, I, I_V, R, R_V \geq 0$. Finally, to consider the subpopulation dynamics in terms of fractions of the entire subpopulation, we set

$$
S + S_V + I + I_V + R + R_V = 1 \tag{2}
$$

and denote d to be the fraction of the never-vaccinated population

$$d = S_D + I_D + R_D.$$

Modeling restrictions

We assume that the VP holders consist of the following subpopulations of vaccinated at least once: V, S_V, I_V, R_V. Recall that the net effect of all non-pharmaceutical interventions is modeled using parameters f_v and f, called restrictions throughout the text. The parameter f_v amounts to the level of restriction of contacts, and thus the ability to infect, within the group of VP holders. The parameter f satisfies $f \geq f_\mathrm{v}$ and corresponds to restriction of contacts within the rest of the population, as well as between the VP holders and the rest of the population.

The restriction level f_v for the VP holders is introduced in the model as a modulator of the transmission rate β_v. Specifically, we assume that $\beta_\mathrm{v} = \beta_0(1 - f_\mathrm{v})$, where β_0 is the transmission rate of the SARS-CoV-2 virus without restrictions. We assume f_v ranges from 0 to 1, where $f_\mathrm{v} = 0$ corresponds to no restrictions enforced on the VP holders, and $f_\mathrm{v} = 1$ corresponding to full restrictions. Given that for $f_\mathrm{v} = 0$ the reproduction number $R_\mathrm{max} = \beta_0/\gamma = 4$, and that the recovery rate $\gamma = 1/6$, we obtain the no-restriction transmission rate $\beta_0 = 2/3$.

Similarly, the transmission rate parameter $\beta = \beta_0(1 - f)$ describes the transmission rate within the rest of the population and between VP holders and the rest, given the restrictions f.

Proportional versus preferential types of social mixing

The above described model equations are based on the assumption that the social mixing between social groups in the population is proportional to the group sizes (the mass action principle). Instead, preferential mixing can be assumed, where the VP holders are more likely to contact other VP holders, since they have lower restrictions [5]. This preferential bias is proportional to the difference between the restrictions f and f_v. To incorporate the preferential mixing effect in the ODE model (Equation 1) we rescale the interaction terms according to the

following rules:

$$
\begin{aligned}
S_V I_V &\rightarrow \frac{\beta_{\mathrm{v}}}{\beta(S+I+R)+\beta_{\mathrm{v}}\left(1-(S+I+R)\right)} S_V I_V \\
S I_V &\rightarrow \frac{\beta}{\beta(S+I+R)+\beta_{\mathrm{v}}\left(1-(S+I+R)\right)} S I_V
\end{aligned}
$$

where $S+I+R$ is the non-immune population.

Model simulations

For simulations, we solve the model numerically by means of joint Adams' and BDF methods, as implemented in the R package deSolve, lsoda method of the ode function [6]. The method monitors data in order to select between non-stiff (Adams') and stiff (BDF) methods. It uses the non-stiff method initially [7].

To generate the data presented in Figure 1b,c, we use the reference setup of parameters: $\beta_0 = 2/3$, $f = 0.63$ (and thus $\beta = 0.247$), $f_{\mathrm{v}} = 0.05$ (and thus $\beta_{\mathrm{v}} = 0.634$), $\gamma = 1/6$, $\kappa = 1/500$, $a = 0.9$, $\upsilon = \upsilon_r = 1/250$, $\omega = 1/500$, $d = 0.1$, with initial conditions $I = 10^{-6}$, $I_D = d \cdot I = 10^{-7}$; $I_N = (1-d) \cdot I = 0.9 \cdot 10^{-6}$, $R = 0$, $V = 0$. Given $I(t)$ resulting from the solution of the model's ODE system, to present the final results as easier interpretable cases per milion rather than fractions, we re-scale the results by 1M. Additionally, we compute a proxy for the daily incidence number of new cases from the following relation between $I\,(t)$ and $I^*\,(t)$:

$$
\begin{aligned}
I\,(t) &= \int_0^t e^{-\gamma(t-\tau)} I^*\,(\tau)\, d\tau \\
&= \int_{t-1}^t e^{-\gamma(t-\tau)} I^*\,(\tau)\, d\tau + e^{-\gamma} \int_0^{t-1} e^{-\gamma(t-1-\tau)} I^*\,(\tau)\, d\tau \\
&\simeq \frac{1}{\gamma} I^*\,(t) \left(1-e^{-\gamma}\right) + e^{-\gamma} I\,(t-1)\,.
\end{aligned}
$$

Thus, the $I^*(t)$ is computed as

$$
I^*(t) \simeq \frac{\gamma}{1-e^{-\gamma}} \left(I(t) - e^{-\gamma} I(t-1)\right).
$$

We proceed similarly to obtain daily incidence numbers I_1^*, I_2^* and for the sum of all infected, and again to make it interpretable in the figures we re-scale it by 1M.

Stability analysis

The vaccination dynamics can be solved explicitly in the absence of infections. Fixing $I = I_V = R = R_V = 0$, and assuming $\upsilon = \upsilon_r$, we obtain

$$\begin{aligned} S(t) &= d + (1-d)\, e^{-\upsilon t}, \\ V(t) &= (1-d)\, \frac{\upsilon a}{\upsilon a + \omega} \left(1 - e^{-(\upsilon a + \omega)t}\right), \\ S_V(t) &= 1 - S - V. \end{aligned}$$

For convenience, where it is not needed, we drop the time argument.

Taking an adiabatic approach we linearize the infection dynamics for small I, I_V and R under the assumption of slowly varying S, S_V and V. In that case, the infection dynamics decouples from the vaccination dynamics and the Jacobian submatrix J_{sub} for the equations for I and I_V is given by:

$$J_{sub} = \begin{pmatrix} \beta S - \gamma & \beta S \\ \beta S_V & \beta_V S_V - \gamma \end{pmatrix}.$$

Given the Jacobian submatrix, we can approximate the dynamics in a small neighborhood of the $I = I_V = 0$ state as

$$\begin{pmatrix} \frac{d}{dt} I \\ \frac{d}{dt} I_V \end{pmatrix} = \begin{pmatrix} \beta S - \gamma & \beta S \\ \beta S_V & \beta_{\mathrm{v}} S_V - \gamma \end{pmatrix} \cdot \begin{pmatrix} I \\ I_V \end{pmatrix}. \tag{3}$$

The instantaneous reproduction number R^* and the instantaneous doubling time D

Since the largest and the second largest eigenvalues $\lambda_{\max}$ and λ_2 of J_{sub} are both real, the solution to Equation 3 providing the dynamics of infection numbers of the vaccinated and the

rest of the population in time can be written in the following form

$$\begin{pmatrix} I(t) \\ I_V(t) \end{pmatrix} = c_1 w_1 e^{\lambda_{\max} t} + c_2 w_2 e^{\lambda_2 t} = e^{\lambda_{\max} t}(c_1 w_1 + c_2 w_2 e^{(\lambda_2 - \lambda_{\max})t}), \tag{4}$$

where w_1 and w_2 are the respective eigenvectors, and c_1 and c_2 are constants depending on the initial conditions.

Since we have $\lambda_2 - \lambda_{\max} \leq 0$, we can approximate the time evolution of infection numbers by

$$\begin{pmatrix} I(t) \\ I_V(t) \end{pmatrix} \approx c_1 w_1 e^{\lambda_{\max} t}. \tag{5}$$

The largest eigenvalue of J_{sub} is given by

$$\lambda_{\max} = \frac{1}{2} S\beta - \gamma + \frac{1}{2} S_V \beta_{\mathrm{v}} + \frac{1}{2}\sqrt{S^2\beta^2 + S_V^2 \beta_{\mathrm{v}}^2 - 2SS_V\beta\beta_{\mathrm{v}} + 4SS_V\beta^2}, \tag{6}$$

whereby it is convenient to express $\lambda_{\max}$ as a function of $R_1 = \frac{\beta}{\gamma}$ and $R_2 = \frac{\beta_{\mathrm{v}}}{\gamma}$. We then obtain

$$\lambda_{\max} = \gamma \left(\frac{1}{2}\left(R_1 S + R_2 S_V\right) + \frac{1}{2}\sqrt{\left(R_1 S - R_2 S_V\right)^2 + 4SS_V R_1^2} - 1 \right). \tag{7}$$

Given the population fractions $S(t)$ and $S_V(t)$ at a given time instant t, the linearized dynamics of infections given by Equation 3 has a corresponding two-type Galton-Watson branching process, which is a microscopic description of the dynamics. The two types of the process correspond to the I and I_V groups. The type I individuals generate $Pois\left(R_1 S\right)$ offsprings of type I and $Pois\left(R_1 S_V\right)$ offsprings of type I_V. The type I_V individuals generate $Pois\left(R_1 S\right)$ offsprings of type I and $Pois\left(R_2 S_V\right)$ offsprings of type I_V. The linearized dynamics (3) can then be understood as a mean field limit of the microdynamics described by such a branching process. Moreover, the spectral norm

$$R^* = \frac{1}{2}\left(R_1 S + R_2 S_V\right) + \frac{1}{2}\sqrt{4R_1^2 SS_V + \left(R_1 S - R_2 S_V\right)^2} \tag{8}$$

of the transition matrix

$$\begin{pmatrix} R_1 S & R_1 S_V \\ R_1 S & R_2 S_V \end{pmatrix}$$

of the branching process can be interpreted as the reproduction number of the branching process, since the expected number of infected in generation n grows like $const \cdot (R^*)^n$ [8]. We refer to R^* as the instantaneous reproduction number. The term instantaneous comes from the fact that we are considering the linearized adiabatic dynamics in a small neighborhood of the $I = I_V = 0$ (ref Eq. 3).

The above discrete branching process can be extended to a continuous time branching process by assuming a probability distribution on the generation time, denoted $\varphi(\gamma)$. The growth of the continuous time branching process $const \cdot e^{\alpha t}$ is characterized by its Malthusian growth parameter, denoted α. The relation between the instantaneous reproduction number R^*, the distribution $\varphi(\tau)$ and the Malthusian parameter α for such a branching process is given by

$$R^* \cdot \mathcal{L}_\varphi(\alpha) = 1$$

where $\mathcal{L}_\varphi(\alpha)$ is the Laplace transform $\int_0^\infty e^{-\alpha\tau}\varphi(\tau)\,d\tau$ of the distribution φ [8]. Since the setting of ODE model (1) implies exponential distribution of the generation time, i.e, $\varphi(\gamma) = Exp(\gamma)$, the following relation holds: $\alpha = \gamma(R^* - 1)$.

By Equation 5, the Malthusian parameter α for our dynamics is given by the largest eigenvalue $\lambda_{\max}$. Hence we obtain the relation between the instantaneous reproduction R^* and the $\lambda_{\max}$ as $\lambda_{\max} = \gamma(R^* - 1)$. Note that since both S and S_V are functions of time, so are $\lambda_{\max}$ and R^*.

It is noteworthy that in the above equations, all R_1, R_2, $R_1 S$ and $R_2 S_V$, and R^* should be seen as reproduction numbers, but of a different nature [9]. R_1 and R_2 are reproduction numbers taking into account the restrictions f and f_{v}, respectively. The $R_1 S$ and $R_2 S_V$ are also group specific, but in addition incorporate the respective group sizes. Finally, R^* combines all these factors together.

Having this and Equation 5, we define the instantaneous doubling time at time, denoted t $D(t)$, as the solution D of $e^{\gamma(R^*(t)-1)\cdot D} = 2$. Such obtained doubling times are featured in Figure 2b.

The times of transitions between subcritical and overcritical epidemics

The analysis of the linearized dynamics around $I = I_V = 0$ allows us to determine transitions between subcritical and overcritical epidemics. Such transitions occur at the time instants t at which $\lambda_{\max}(t) = 0$, or, equivalently, at $R^*(t) = 1$. We thus find that for given values of $S(t)$ and $S_V(t)$ the critical times t for transitions between subcritical and overcritical epidemics are the roots of the equation

$$\lambda_{\max}(t) = 0.$$

The obtained critical threshold times are plotted in the lower triangles of the panels in Figure 3 in the main text. In the case of proportional mixing the above equation is equivalent to:

$$(R_1 S(t) - 1)\,(R_2 S_V(t) - 1) = R_1^2 S(t) S_V(t).$$

Asymptotic structure of the population

The asymptotic structure of the population in terms of the sizes of the subpopulations V, S_V and S_D can be easily obtained by setting $I = I_V = R = R_V = 0$ and computing the stable stationary solution for V^{as}, S^{as} and S_V^{as} of our ODE system (1):

$$\begin{aligned} S^{\text{as}} &= d \\ S_V^{\text{as}} &= (1-d)\,(1-\eta) \\ V^{\text{as}} &= (1-d)\eta \\ S^{\text{as}} + S_V^{\text{as}} &= 1 - V^{\text{as}}, \end{aligned}$$

where

$$\eta = \frac{a}{1 + \omega/\upsilon_r}$$

can be seen as the actual immunization rate in the population, and is expressed as a function of vaccine effectiveness a and the ratio of the immunity waning rate ω and the revaccination rate υ_r. The obtained values correspond to the structure in the limit $t \to \infty$ and represent the structure to which the population converges in the long term.

Having this, we obtain the asymptotic instantaneous reproduction number R^* by inserting the asymptotic values S^{as} and S_V^{as} into Equation 8. These values are plotted in the upper triangles in the panels of Figure 3 in the main text.

Finally, we solve for such minimum common restrictions $f = f_{\text{v}} = f_{\text{min}}$, which will result in instantaneous reproduction number $R^* = 1$ for the different vaccine effectiveness and vaccination rate setups. Hence f_{min} is found from $R_{\text{max}}\,(1 - f_{\text{min}}) = 4\,(1 - f_{\text{min}}) = \frac{1}{1-V}$ as

$$f_{\text{min}} = \max\left(0, 1 - \frac{1}{4(1 - V^{\text{as}})}\right).$$

Model limitations

VAP-SIRS is not compartmentalized for age groups and does not consider deaths or healthcare system limitations like some other models, albeit in the context of exploring different parameters than larger freedom for VP holders [10, 11, 12, 13, 14, 15]. Deaths could be taken into account through a straightforward modification of the model, which would however lead to more parameters. In this case, the fact that vaccination reduces the risk of death would have to be accounted for. The impact of deaths on public health and society, which is very important especially when the epidemic becomes overcritical, can be indirectly assessed based on the number of infection cases. In general, features such as age groups and deaths, however, do not add further insights into the questions which are the focus of our study, namely, the long-term effects of VPs and avoiding overcritical dynamics. In this context, the advantage of our model is that it is enriched in features such as revaccinations and waning immunity, which are particularly relevant in the long term.

Nevertheless, possible extensions to our model could include inter- individual or age-dependent variations in immunity, which is also relevant for people with severe chronic conditions or immunodeficiencies, or changes in behaviour over time. The presented analysis has been performed assuming that without restrictions, the maximum reproduction number of the virus is $R_{max} = 4$. More transmittable variants could easily be modeled by fixing higher values of R_{max}. Similarly, our results do not account for the possibility of immune escape variants, but such variants could be considered using our model by fixing smaller vaccine effectiveness than

the values we considered. Asymptotic endemic states of the ODE system (1) could easily be computed, but are not discussed here due to space constraints. Finally, another limitation of our analysis is that not all parameter values are exactly known, such as the post- vaccination or natural immunity waning time. We, however, fix optimistic values for such parameters, and show that unfavorable infection dynamics can still be obtained even under optimistic assumptions.

Data Availability

Not applicable

Code Availability

The VAP-SIRS model was implemented using R version 4.0.2 along with the shiny package to build an interactive web application that allows to simulate the model. The code of the model is available online in the GitHub repository: https://github.com/storaged/VAP-SIRS, and the on-line tool is available http://bioputer.mimuw.edu.pl:85/VAP-SIRS/. The code to generate Fig 2 and Fig 3 from the main text is available at https://github.com/eMaerthin/Fig2_Fig3.

References

1. Keeling, M. J. & Rohani, P. *Modeling Infectious Diseases in Humans and Animals* (Princeton University Press, 2011).
2. Tarke, A. *et al.* Negligible impact of SARS-CoV-2 variants on CD4+ and CD8+ T cell reactivity in COVID-19 exposed donors and vaccinees. *bioRxiv*. https://www.biorxiv.org/content/early/2021/03/01/2021.02.27.433180 (2021).
3. Chia, W. N. *et al.* Dynamics of SARS-CoV-2 neutralising antibody responses and duration of immunity: a longitudinal study. *The Lancet Microbe* (2021).
4. Zuo, J. *et al.* Robust SARS-CoV-2-specific T cell immunity is maintained at 6 months following primary infection. *Nature Immunology* (2021).

5. Marschner, I. C. The effect of preferential mixing on the growth of an epidemic. *Mathematical Biosciences* **109,** 39–67 (1992).

6. Soetaert, K., Petzoldt, T. & Setzer, R. W. Solving Differential Equations in R: PackagedeSolve. *Journal of Statistical Software* **33** (2010).

7. Hindmarsh, A. C. & Petzold, L. R. Algorithms and software for ordinary differential equations and differential- algebraic equations, Part II: Higher-order methods and software packages. *Computers in Physics* **9,** 148 (1995).

8. Athreya, K. B. & Ney, P. E. *Branching Processes* German. OCLC: 863789203 (1972).

9. Van den Driessche, P. Reproduction numbers of infectious disease models. *Infectious Disease Modelling* **2,** 288–303 (2017).

10. Sadarangani, M. *et al.* Importance of COVID-19 vaccine efficacy in older age groups. *Vaccine* **39,** 2020–2023 (2021).

11. Moore, S., Hill, E. M., Tildesley, M. J., Dyson, L. & Keeling, M. J. Vaccination and non-pharmaceutical interventions for COVID-19: a mathematical modelling study. *The Lancet Infectious Diseases* (2021).

12. Jentsch, P. C., Anand, M. & Bauch, C. T. Prioritising COVID-19 vaccination in changing social and epidemiological landscapes: a mathematical modelling study. *The Lancet Infectious Diseases* (2021).

13. Bubar, K. M. *et al.* Model-informed COVID-19 vaccine prioritization strategies by age and serostatus. *Science* **371,** 916–921 (2021).

14. Bauer, S. *et al.* Relaxing restrictions at the pace of vaccination increases freedom and guards against further COVID-19 waves in Europe. *arXiv:2103.06228 [q-bio].* arXiv: 2103.06228. http://arxiv.org/abs/2103.06228 (2021).

15. Giordano, G. *et al.* Modeling vaccination rollouts, SARS-CoV-2 variants and the requirement for non-pharmaceutical interventions in Italy. *Nature Medicine* (2021).

End notes

Acknowledgements

SC acknowledges support by University of Malta. TC has received funding from the European Union's Horizon 2020 research and innovation programme under grant agreement No 101016233 (PERISCOPE) GG acknowledges support by the University of Trento within the COVID-19 Strategic Project MOSES (Models for Reasoning about the Spreading of Diseases). MP was supported by the Slovenian Research Agency (Grant Nos. P1-0403 and J1-2457). EP acknowledges support by the University of Crete. ES acknowledges funding by the Polish National Science Centre OPUS grant no 2019/33/B/NZ2/00956 and SONATA-BIS grant no 2020/38/E/NZ2/00305.

Author contributions

AG, KG, TK, and ES conceived the VAP-SIRS model - with input and feedback on the model and results from TC, GG, MP, EP and MR. TK performed the stability analysis. KG implemented model simulations and the Shiny application for visualizations. MB implemented the stability analysis. SC, TC, EP, and MR performed literature search. ES supervised the study. All authors wrote and provided critical feedback to the manuscript.

Competing interests

Other projects in the research lab of ES are co-funded by Merck Healthcare KGaA .

Additional information

Correspondence and requests for materials should be addressed to ES. Reprints and permissions information is available at www.nature.com/reprints.

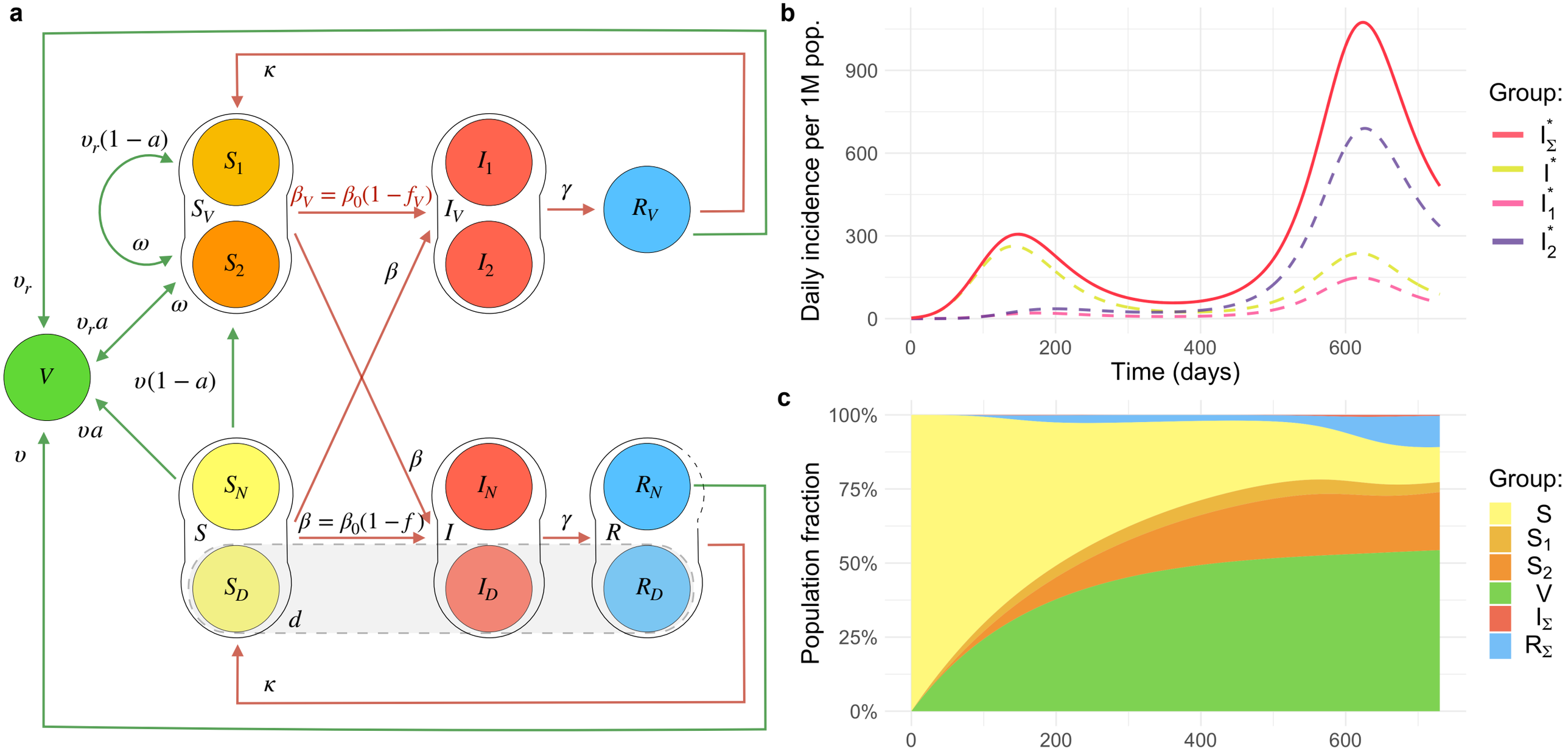
a
κ
$v_r(1-a)$
S_1
S_V
S_2
ω
$\beta_V = \beta_0(1-f_V)$
I_1
I_V
I_2
γ
R_V
β
v_r
$v_r a$
ω
V
$v(1-a)$
va
v
S_N
S
S_D
d
$\beta = \beta_0(1-f)$
β
I_N
I
I_D
γ
R_N
R
R_D
κ
b
Daily incidence per 1M pop.
900
600
300
0
0
200
400
600
Time (days)
Group:
I^*_Σ
I^*
I^*_1
I^*_2
c
Population fraction
100%
75%
50%
25%
0%
0
200
400
600
Group:
S
S_1
S_2
V
I_Σ
R_Σ

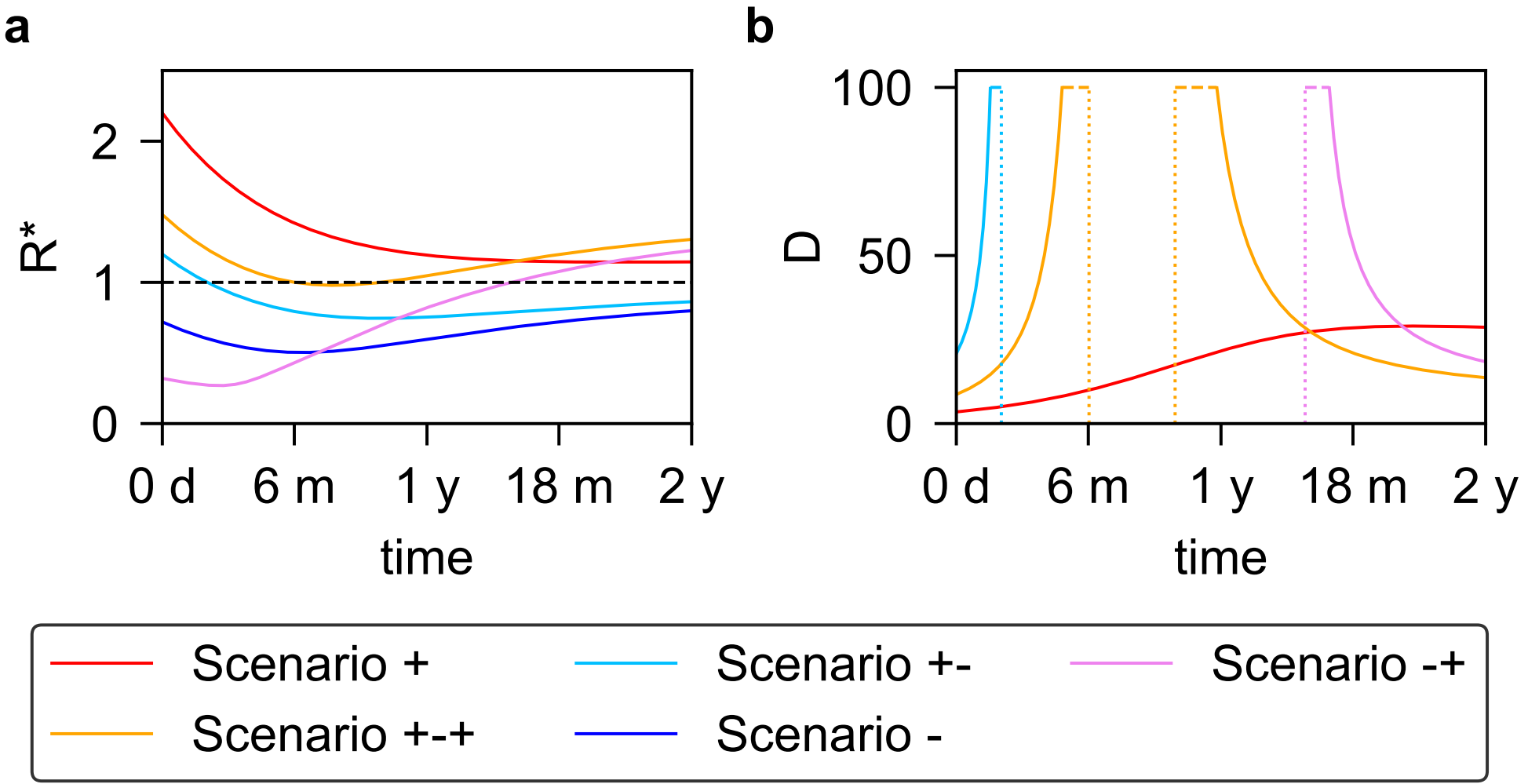
a
b
R*
2
1
0
0 d
6 m
1 y
18 m
2 y
time
D
100
50
0
0 d
6 m
1 y
18 m
2 y
time
Scenario +
Scenario +-
Scenario -+
Scenario +-+
Scenario -

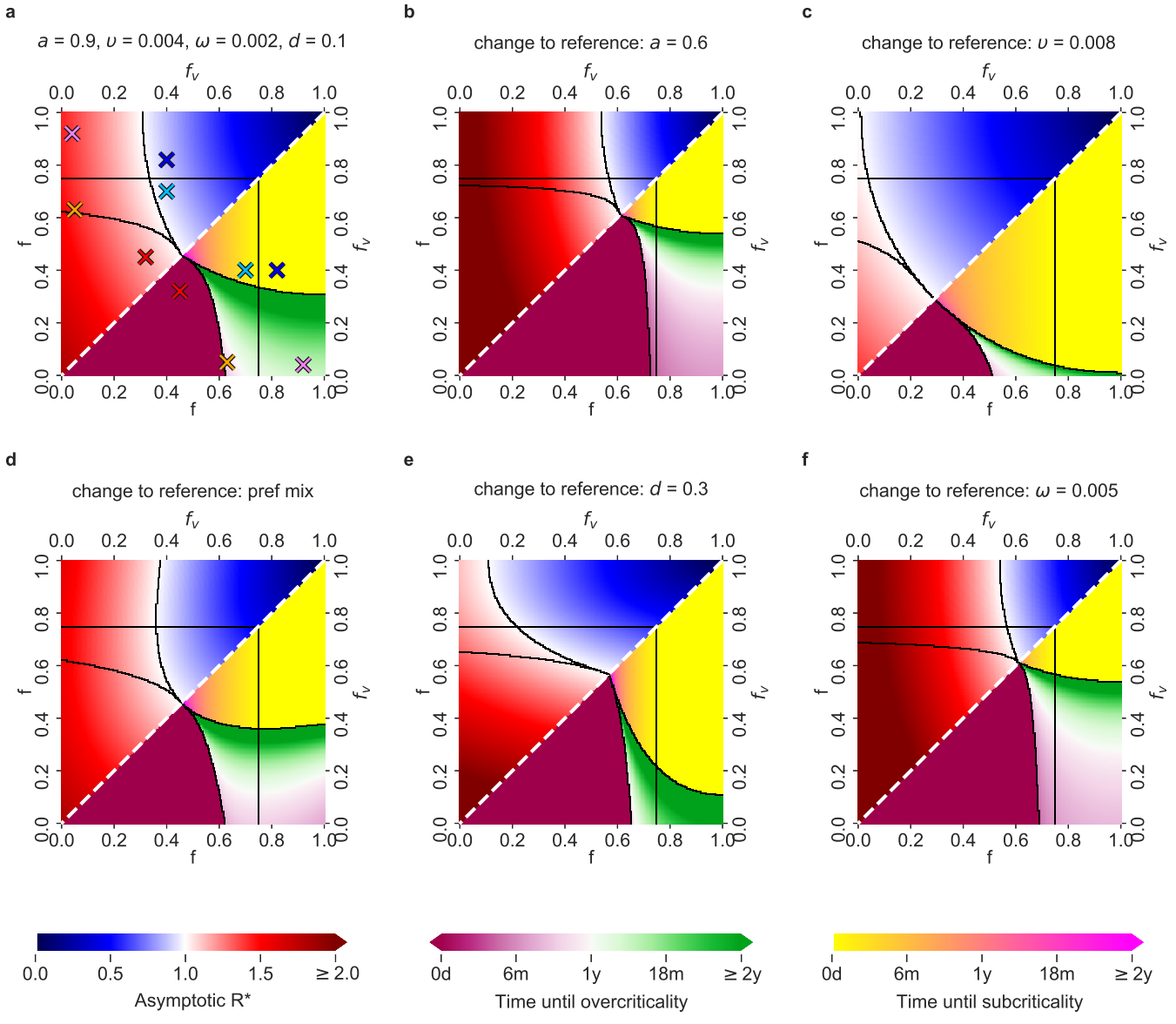
a
a = 0.9, υ = 0.004, ω = 0.002, d = 0.1
b
change to reference: a = 0.6
c
change to reference: υ = 0.008
d
change to reference: pref mix
e
change to reference: d = 0.3
f
change to reference: ω = 0.005
f
f_v
0.0 0.2 0.4 0.6 0.8 1.0
0.0 0.5 1.0 1.5 ≥ 2.0
Asymptotic R*
0d 6m 1y 18m ≥ 2y
Time until overcriticality
Time until subcriticality